Translational Oncology 16 (2022) 101309

Contents lists available at ScienceDirect

Translational Oncology

journal homepage: www.elsevier.com/locate/tranon

Original Research

Chimeric antigen receptor T cells targeting CD147 for non-small cell lung cancer therapy

Xiao-Hong Chen [1], Ruo Chen [1], Ming-Yan Shi [1], Ruo-Fei Tian, Hai Zhang, Zhi-Qian Xin, Zhi-Nan Chen [*], Ke Wang [*]

National Translational Science Center for Molecular Medicine and Department of Cell Biology, Fourth Military Medical University, Xi'an 710032, China

ARTICLE INFO

Keywords:
CART
CD147
NSCLC
Immunotherapy

ABSTRACT

Non-small cell lung cancer (NSCLC) is a highly malignant tumor, with a significant mortality and morbidity. With the development of tumor immunotherapy, chimeric antigen receptor T cells (CART) gets increasingly attention and achieves prominent contributions in the treatment of hematologic malignancies. However, CART therapy for NSCLC proceeds slowly and further researches need to be investigated. In our study, we performed bioinformatics analysis to evaluate the significant role of CD147 in NSCLC. The expression level of CD147 was detected in human NSCLC cell lines and NSCLC tissues. Meanwhile, CD147-CART was constructed and identified. Cell cytotoxicity and cytokine secretion were performed to evaluate the efficacy of CD147-CART. We also constructed cell-derived xenograft (CDX) model and patient-derived xenograft (PDX) model, which was used to further investigate the safety and efficacy of CD147-CART *in vivo*. Our observations show that CD147 is a specific tumor antigen of NSCLC and plays an essential role in NSCLC progression, which can be used as a target for CART therapy in NSCLC. CD147-CART cells exhibit robust cytotoxicity and cytokine production *in vitro*, suggesting a strong anti-tumor activity against NSCLC tumor cells. Importantly, CD147-CART cells have strong anti-tumor activity against NSCLC cells *in vivo* in both CDX and PDX models and no adverse side effects. Our findings show that CD147-CART immunotherapy for NSCLC is safe and effective, which is an ideal and promising medical patch for treating NSCLC.

Background

Recently, the incidence of cancer has been increasing gradually, which threatens human health seriously [1–3]. Data from the World Health Organization shows that the mortality (18%) and morbidity (11.4%) rates of lung cancer occupies the first or second position in malignant tumors around the world [3]. NSCLC accounts for approximately 85% of lung cancer, lung adenocarcinoma (LUAD) and lung squamous cell carcinoma (LUSC) mainly included [4]. Despite rapid improvements in NSCLC treatment, including surgery, chemo-radiotherapy, and targeted therapy, the recurrence and 5-year survival rate are still suspenseful [5–10]. Therefore, it is necessary to develop novel treatments for NSCLC patients to improve survival and quality of life.

With the development of tumor immunology, immunotherapy gets increasingly attention and achieves prominent contributions in cancer treatment, including cytotoxic T-lymphocyte antigen-4 (CTLA-4) inhibitors, programmed death-1 (PD-1) inhibitors, CART, dendritic cell vaccine, and cytokine-induced killer cells [11–13]. As a novel adoptive immunotherapy, CART cell therapy has developed rapidly and more than 100 clinical trials are ongoing worldwide [14,15]. CART cells specifically recognize tumor antigens and are rapidly activated to kill tumor cells. Currently, CART therapy is mainly used in the treatment of hematologic malignancies. Two CART products targeting CD19,

Abbreviations: NSCLC, non-small cell lung cancer; CART, chimeric antigen receptor T cells; CDX, cell-derived xenograft; PDX, patient-derived xenograft; LUAD, lung adenocarcinoma; LUSC, lung squamous cell carcinoma; CTLA-4, cytotoxic T-lymphocyte antigen-4; PD-1, programmed death-1; MHC, major histocompatibility complex; scFv, single-chain variable fragment; TCGA, the Cancer Genome Atlas; GO, Gene ontology; KEGG, Kyoto Encyclopedia of Genes and Genomes; OS, overall survival; FFLuc, firefly luciferase; IHC, immunohistochemistry; PBMCs, peripheral blood mononuclear cells; LDH, lactate dehydrogenase; H&E, hematoxylin & eosin; BMI, bioluminescence imaging; E:T ratios, effector : target ratios; DEGs, differentially expressed genes; PCA, principal component analysis.

* Corresponding authors.
E-mail addresses: znchen@fmmu.edu.cn (Z.-N. Chen), wangke@fmmu.edu.cn (K. Wang).

[1] These authors contributed equally to this work.

https://doi.org/10.1016/j.tranon.2021.101309
Received 21 October 2021; Received in revised form 23 November 2021; Accepted 6 December 2021

Kymriah and Yescarta, have been approved by the Food and Drug Administration for the treatment of relapsed and refractory acute lymphoblastic leukemia and relapsed specific large B-cell lymphoma, which show a good therapeutic effect [10,16]. However, the therapeutic effect of CART in solid tumors, including NSCLC, is poor due to lack of tumor-specific antigens, antigen heterogeneity, immunosuppressive tumor microenvironment, and low levels of infiltration of CART cells into tumor tissue [17]. Currently, most tumor-associated antigens are used as targets for CART therapy in NSCLC patients, including EGFR, MSLN, MUC1, and PSCA, which contributes to on-target/off-tumor and cellular toxicity [17]. The unique technical advantages of CART cell therapy, including no limitation of MHC antigen presentation, short preparation time *in vitro* and immune memory potential, are expected and desired in the field of solid tumor therapy [18,19]. Therefore, the further investigation on CART cells for NSCLC treatment is urgently needed to overcome obstacles.

The tumor-associated antigen CD147, a highly glycosylated transmembrane immunoglobulin, is widely and specifically expressed in multiple malignancies, including hepatocellular carcinoma, NSCLC, glioma, and breast cancer [20]. CD147 is reported to be positively associated with tumor proliferation, invasion, metastasis, and tumor angiogenesis [21–24]. Two drugs targeting CD147, Licartin [25] and Metuzumab [26], demonstrate a good therapeutic effect in the treatment of hepatocellular carcinoma and NSCLC, respectively. Therefore, CD147 is considered as a potential and promising target for CART therapy.

In our study, we found that CD147 was a specific tumor antigen of NSCLC and played an essential role in NSCLC progression, which could be used as a target for CART therapy in NSCLC. *In vitro and in vivo* experiments showed that CD147-CART cells exhibited a strong anti-tumor activity against NSCLC tumor cells. Our findings show that CD147-CART immunotherapy for NSCLC is safe and effective, which provides a promising target and drives the clinical development for NSCLC treatment.

Methods

Bioinformatic analysis

The mRNA data of NSCLC (LUAD, tumor tissues, 519 samples, tumor-adjacent tissues, 58 samples; LUSC, tumor tissues, 497 samples, tumor-adjacent tissues, 49 samples) was obtained from the Cancer Genome Atlas (TCGA) database (https://cancergenome.nih.gov). In order to explore the role of CD147 in the NSCLC progression, the tumor samples were selected and divided into three groups according to quartile, including high CD147 group (> 75%), moderate CD147 group (25%-75%), and low CD147 group (< 25%). The differentially expressed genes (DEGs) between high CD147 group and low CD147 group were identified according to the role of $P < 0.05$, $|\log_2(\text{Foldchange})| > \log_2(1.5)$. Gene ontology (GO) enrichment analysis and Kyoto Encyclopedia of Genes and Genomes (KEGG) analysis were performed using clusterProfile software (Version 4.02). The overall survival (OS) analysis was operated using Gene Expression profiling Interactive Analysis (GEPIA) (http://gepia.cancer-pku.cn/) [27] and the Kaplan Meier Plotter (https://kmplot.com/analysis/) [28]. TIMER (https://cistrome.shinyapps.io/timer/) analysis was performed to explore the correlation between CD147 expression and CD8+ T cell infiltration [29,30].

Vector design

The lentivirus encoding CD147-CAR gene was obtained from Genechem Co.,Ltd.. CD147-CAR vector was mainly composed of anti-CD147 single-chain variable fragment (scFv), CD8 hinge, 4–1BB costimulatory domain, and CD3ζ signaling domain. Anti-CD147 scFv was acquired from the sequences of humanized monoclonal antibody against CD147 (WBP247, produced by our laboratory), and then fused to a human CD8 hinge, a 4–1BB cytoplasmic domain, and a CD3ζ signaling domain to construct CD147-CAR. The CD147-CAR gene was cloned into the vector (Genechem) using *Bam*HI/EcoRI.

Cell lines

The NSCLC cell line A549 was obtained from the American Type Culture Collection, and H460, H1975, and H2170 cell lines were purchased from the Cell bank of Chinese Academy of Sciences. The cell lines A549 and H460 were transfected with lentiviral vector encoding firefly luciferase (FFLuc) gene to generate A549-FFLuc and H460-FFLuc cell lines. All cell lines were cultured at 37 °C under 5% CO_2 in RPMI 1640 medium (10–040-CVRC, CORNING) which was supplemented with 10% fetal bovine serum (10,100–147, Gibco), 2% L-glutamine, and 1% penicillin/streptomycin. Meanwhile, the cell lines have been tested and authenticated using Short Tandem Repeat DNA profiling by Beijing Microread Genetics Co., Ltd. (Beijing, China).

Western blotting

The total protein was extracted from A549, H2170, H460, and H1975 cells using RIPA lysis buffer (P0013B, Beyotime), and was quantified by BCA Protein Assay Kit (23,225, Thermo Fisher Scientific). After adding 5 × loading buffer, the samples were heated at 100 °C for 5–10 min and loaded onto 10% SDS-PAGE gel for electrophoresis. Then, they were transferred to PVDF membranes (IPVH00010, Millipore) followed by 5% non-fat milk for 1 h. Subsequently, the membranes were incubated at 4 °C overnight with the corresponding primary antibodies (anti-CD147 antibody (HAb18) [31,32], produced in our laboratory; anti-CD147 antibody, 13287S, CST; anti-β-actin antibody, M1210–2, HUABIO). After washed with TBST, PVDF membranes were incubated at room temperature for 1 h with goat anti-mouse IgG ($H + L$) antibody (31,430, Thermo Fisher Scientific). Finally, the membranes were washed with TBST and the images were obtained from imaging system (BIO-RAD).

Flow cytometry

The cells were collected and incubated with the corresponding antibodies (PE/Cyanine7 anti-human CD147 antibody, 306,216, BioLegend; FITC anti-human CD3 antibody, 300,406, BioLegend; APC/Cyanine7 anti-human CD4 antibody, 317,418, BioLegend; PerCP/Cyanine5.5 anti-human CD8a antibody, 301,032, BioLegend; FITC-Labeled Recombinant Protein L, RPL-PF141, ACRO Biosystems; PE anti-human CD25 antibody, 302,606, BioLegend; APC anti-human CD69 antibody, 310,910, BioLegend; APC anti-human CD107a antibody, 328,619, BioLegend; PE/Cyanine7 anti-human PD-1 antibody, 329,917, BioLegend; PerCP/Cyanine5.5 anti-human CD8a antibody, 301,032, BioLegend; PE-anti human IL-2 antibody, 500,307, BioLegend; PE/Cyanine7 anti-human IFN-γ antibody, 502,528, BioLegend; APC anti-human TNF-α antibody, 502,912, BioLegend) at 4 °C for 30 min. After washed with PBS, all samples were detected by FACS Aria instrument (BD Biosciences) and data were analyzed with FlowJo7.6 software (Tree Star).

Immunohistochemistry (IHC) analysis

IHC staining was performed using a General SP kit (SP-9000, ZSGB-BIO) according to manufacturer's protocol and 3,3′-diaminobenzidine (ZLI-9019, ZSGB-BIO). Cell nucleus was stained by hematoxylin (G1140, Solarbio). For the detection of CD147 expression in NSCLC tissues, tissue microarrays of LUAD and LUSC were purchased from Shanghai Outdo Biotech, anti-CD147antibody (HAb18) was used to detect the expression of CD147 in NSCLC tissue microarrays. For tumor tissues from CDX model or PDX model, the corresponding primary antibodies (anti-Ki67 antibody, ab16667, Abcam; anti-CD3 antibody, ab5690, Abcam; anti-

CD8α antibody, ab237709, Abcam) were used to detect the targeted proteins. Cell apoptosis in tumor tissues was evaluated using TUNEL Assay Kit (ab206386, Abcam) according to manufacturer's instruction.

Peripheral blood mononuclear cells (PBMCs) isolation and CD147-CART construction

PBMCs were isolated from healthy donors by Ficoll-Hypaque density-gradient centrifugation and cultured in 24-well plate with 2 μg/ml anti-human CD3 antibody (317,347, BioLegend), 4 μg/ml anti-human CD28 antibody (302,943, BioLegend), and 200 IU/ml recombinant human IL-2 (200–02, PeproTech). After two days, PBMCs (1×10^6 cells) were transfected with lentivirus (Genechem) encoding CD147-CAR gene, and the culture was supplemented with 200 IU/mL recombinant human IL-2 every 48 h. The subtype and phenotype of CD147-CART cells were identified with flow cytometry analysis, which was described in the methods of flow cytometry.

Lactate dehydrogenase (LDH) release assay

The cell lines A549, H2170, and H460 were co-cultured with CD147-CART cells or PBMCs in 96-well plate for 6 h according to different effector: target (E:T) ratios. The supernatant was collected and detected by the Cytotoxicity Detection Kit^{PLUS} (LDH) (4,744,934,001, Roche) according to the manufacturer's protocol. The calculation of% cell lysis from the LDH release assay was performed using the following equation: Cytotoxicity (%) = (exp. value – low control)/(high control – low control) × 100%.

Firefly luciferase reporter system assay

The cell lines A549-FFLuc and H460-FFLuc were co-cultured with CD147-CART cells or PBMCs in 96-well plate at the indicated E: T ratios. After 6 h, the live tumor cells were determined by Dual Luciferase Reporter Assay System Kit (E1980, Promega). The cell lysis (%) was calculated using the formula, 1-(experimental signal/maximal signal) × 100%.

Cytokine secretion assay

The NSCLC cells (A549, H2170, and H460) were co-cultured with CD147-CART cells or PBMCs in 96-well plate for 6 h according to different E:T ratios. The supernatant was collected and analyzed using AimPlex Human Th1/Th2/Th17 7-Plex Kit (C191107, QuantoBio). All samples were detected by FACS Aria instrument (BD Biosciences) and data were analyzed with FCAP Array Software V3.0 (BD Biosciences).

Xenograft model for CD147-CART treatment

BALB/c nude mice (6–8 weeks, female) were purchased from Beijing Vital River Laboratory Animal Technology Co., Ltd.. All procedures were approved by the Animal Care and Use Committee of Fourth Military Medical University. For CDX model, the mice ($n = 15$) were injected subcutaneously with 2×10^6 A549-FFluc cells in 100 μl sterile PBS. After two weeks, the mice were averagely divided into three groups according to the tumor size. One group of mice received only 2×10^6 PBMCs suspended in 50 μl PBS, one group with 2×10^6 CD147-CART cells suspended in 50 μl PBS, those in the control group underwent the same injection with 50 μl PBS simultaneously. The treatment was performed by intratumoral injection twice a week for a total of four times. Meanwhile, mouse weight and tumor volume were measured every two days. The tumor size was calculated as follows: tumor size (mm^3) = (length × $width^2$)/2. At day 1, 8 and 13, each mouse was injected with 150 mg/kg D-Luciferin potassium salt (ST196, Beyotime) intraperitoneally for bioluminescence imaging (BMI). The images were recorded using a IVIS Lumina II (PerkinElmer). After the end of the treatment, all the mice were sacrificed after anesthesia and tissues were used to perform hematoxylin & eosin (H&E), IHC staining and flow cytometry. For PDX model, the mice were transplanted subcutaneously with NSCLC tumor tissues obtained from BEIJING IDMO Co., Ltd.. At 42 days post-inoculation, tumor-bearing mice were averagely divided into two groups according to the tumor size, which were treated with 2×10^6 PBMCs and 2×10^6 CD147-CART suspended in 50 μl PBS intratumorally every three days for a total of three times. Mouse weight and tumor volume were measured every two days. After the end of the treatment, all the mice were sacrificed after anesthesia and tissues were used to perform IHC staining.

H&E staining

The tissues of heart, liver, spleen, lung, kidney, and intestines were fixed with 10% paraformal-dehyde, embedded in paraffin, and sectioned at a thickness of 4 μm. After dewaxing, the sections were stained with hematoxylin (G1140, Solarbio) and eosin (BA-4033, Baso).

Statistical analysis

All statistical analyses were performed using GraphPad Prism 9.0 software. All data were presented as mean ± SEM at least three independent experiments. Significant difference was analyzed using unpaired two-tailed Student's *t*-test. OS was calculated using Kaplan-Meier analysis and log-rank test. $P < 0.05$ was considered to denote statistical significance.

Results

Tumor specific antigen CD147 plays a critical role in NSCLC progression

CD147 is reported to be an important tumor-associated antigen in multiple tumors [33,34]. In order to further explore the role of CD147 in NSCLC progression, the data of LUAD and LUSC obtained from TCGA database was performed by bioinformatic analysis. Principal component analysis (PCA) showed a separate trend in tumor samples from the high and low CD147 groups in both LUAD and LUSC tissues (Fig. S1A, B). This result indicated that there existed two different gene expression patterns in the high and low CD147 samples, which was closely related to CD147 expression. In LUAD, a total of 3571 genes was identified as DEGs between the high and low CD147 groups, including 707 up-regulated genes and 2864 down-regulated genes in high CD147 group (Fig. 1A); in LUSC, 3250 genes were screened as DEGs, including 742 up-regulated genes and 2508 down-regulated genes in high CD147 group (Fig. S1C). Then, the top 50 DEGs were selected and exhibited in heat map (Figs. 1B, S1D). GO enrichment analysis and KEGG pathway analysis revealed these DEGs were mainly related to tumor immune response, tumor cell proliferation, and tumor cell metabolism (Figs. 1C, D, S1E, F). TIMER is a comprehensive online resource for systematic analysis of immune infiltrates across diverse cancer types using RNA-Seq expression profiling data [29,30]. The infiltration of CD8+ T cells was assessed by TIMER on NSCLC sample data and the results denoted that the infiltration of CD8+ T cells was negatively associated with CD147 expression in NSCLC (Fig. 1E). GEPIA is a newly developed interactive web server for analyzing RNA-Seq expression data of tumors and normal samples from TCGA and GTEx projects, which provides differential expression analysis and patient survival analysis [27]. OS analysis from GEPIA showed that high CD147 expression predicted a poor prognosis in NSCLC, which is consistent with OS analysis of Kaplan Meier Plotter (Fig. 1F,G). To further explore the role of CD147 expression in NSCLC, the relationship between CD147 expression and clinical characteristics of NSCLC patients was investigated by Kaplan-Meier Plotter. The results revealed that high CD147 expression was significantly related to poor OS in male, female, smoking, no-smoking, stage 1, stage 2, ATCC stage T1, and AJCC stage M0 patients (Table 1).

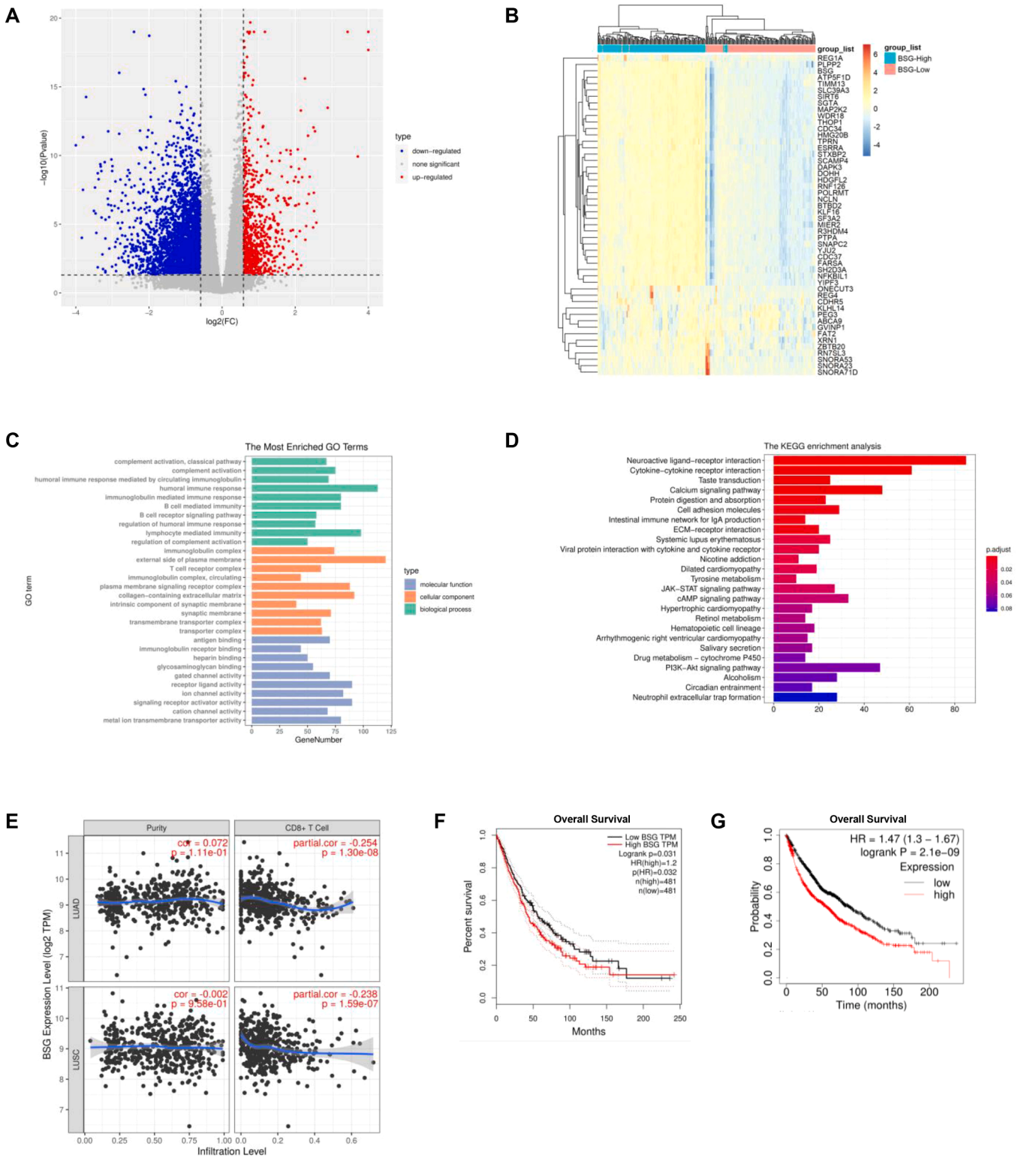

Fig. 1. The role of CD147 in LUAD was evaluated by bioinformatic analysis. **A** The volcano plot showed that 3571 DEGs between high CD147 samples and low CD147 samples were identified in LUAD. **B** The heat map showed the top 50 DEGs between high CD147 samples and low CD147 samples in LUAD. **C** The top 50 DEGs between high CD147 samples and low CD147 samples in LUAD were subjected to GO enrichment analysis according to biological process, cellular component, and molecular function. **D** KEGG enrichment analysis was performed on the basis of the top 50 DEGs between high CD147 samples and low CD147 samples in LUAD. **E** The correlation of CD8+ T cell infiltration and CD147 expression in NSCLC was analyzed by TIMER. **F** OS rates of NSCLC patients with high and low CD147 expression levels were determined by GEPIA. **G** OS rates of NSCLC patients with high and low CD147 expression levels were determined by Kaplan Meier Plotter.

Table 1
Correlation of CD147 mRNA expression and clinical prognosis in NSCLC for different clinicopathological factors.

Clinicopathological Characteristic	Overall survival		
	N	Hazard ratio	P
Gender			
Male	1387	1.41 (1.2 - 1.65)	**2.20E-05**
Female	817	1.43 (1.13 - 1.8)	**0.0027**
Smoking			
Yes	970	1.34 (1.09 - 1.66)	**0.0053**
No	247	4.12 (2.15 - 7.9)	**3.70E-06**
Grade			
I	202	1.39 (0.97 - 2)	0.0693
II	310	1.01 (0.74 - 1.39)	0.9293
III	77	1.3 (0.67 - 2.51)	0.4336
Stage			
1	652	2.22 (1.68 - 2.93)	**9.10E-09**
2	320	1.95 (1.35 - 2.83)	**0.0004**
3	70	0.89 (0.51 - 1.56)	0.6858
4	4	–	–
AJCC Stage T			
1	475	1.36 (1.02 - 1.81)	**0.034**
2	686	1.08 (0.86 - 1.35)	0.5026
3	99	1.37 (0.83 - 2.27)	0.22
4	48	0.87 (0.46 - 1.63)	0.6557
AJCC Stage N			
0	863	1.23 (1 - 1.52)	0.0551
1	296	1.13 (0.83 - 1.55)	0.4387
2	113	0.81 (0.54 - 1.21)	0.2971
AJCC Stage M			
0	818	1.24 (1 - 1.52)	**0.0463**
1	10	–	–

To verify the data from the bioinformatics analysis, the expression of CD147 in NSCLC cell lines was detected by western blotting and flow cytometry (Figs. 2A, B, S2A). IHC analysis was also performed to detect CD147 expression in NSCLC tissues and their tumor-adjacent tissues, the expression level of CD147 was classified with "–", "+", "++" and "+++" in terms of the staining intensity and density of each sample (Fig. 2C). The "–" and "+" levels were defined as low CD147, and '++" and "+++" levels were defined as high CD147. The results showed that CD147 was highly expressed in tumor tissues compared with the tumor-adjacent tissues (Fig. 2D, E). Kaplan-Meier analysis illustrated that high CD147 expression was significantly associated with poor OS in NSCLC ($P = 0.0281$) and LUAD ($P = 0.0139$), while no significant difference was observed in LUSC ($P = 0.7415$) (Fig. 2F–H), which further verified the result of bioinformatic analysis. Therefore, our findings indicate that CD147, a specific tumor antigen, exhibits an essential role in NSCLC progression and is a promising target for CART therapy in NSCLC.

Generation and phenotype of CD147-CART cells

To redirect human T cells to CD147 in NSCLC, we constructed a second generation CD147-CAR lentiviral vector containing anti-CD147 scFv, CD8 hinge, 4–1BB costimulatory domain, and CD3ζ signaling domain (Fig. 3A). PBMCs from healthy donor were activated with anti-CD3 antibody and anti-CD28 antibody for 48 h before transfection with CD147-CAR lentiviral. CART subtypes and transfection efficiency were detected after 5 days by flow cytometry. The results showed that more than 95% of cells were CD3-positive, and more than 35% was CD8-positive (Fig. 3B). The transfection efficiency of CD147-CART cells were highly up to 77% (Fig. 3C). Meanwhile, we examined the phenotype of CD147-CART cells including the activation markers CD25 and CD69, degranulation marker CD107a, and exhaustion markers PD-1 by flow cytometry. Compared with the control, the significant upregulation of CD25 and CD69 was observed in CD147-CART group (Fig. 3D, F), and CD107a and PD-1 expression showed no significant difference in the two groups (Fig. 3E, F). Our findings manifest that CD147-CART cells are successfully constructed, which can be used for further study.

CD147-CART cells specifically kill NSCLC cells in vitro

To evaluate CD147-CART cytotoxicity, the NSCLC cell lines were co-cultured with CD147-CART cells, Mock-T cells or PBMCs in 96-well plate for 6 h according to different E:T ratios. Obvious anti-tumor activities were observed under an inverted microscope, tumor cells were surrounded with more CD147-CART cells compared with PBMCs group, which generated more cell masses (Fig. 4A, B). Consistently, LDH release assays revealed that CD147-CART cells mediated stronger anti-tumor activity than PBMCs against tumor cells, the percentage of A549 cell lysis is approximately 60% at E:T ratio of 8:1; the percentage of H460 cell lysis is approximately 90% at E:T ratio of 8:1; and the percentage of H2170 cell lysis is approximately 100% at E:T ratio of 20:1 (Fig. 4C). In addition, the PBMC and Mock-T cell groups showed no significant difference in anti-tumor activity (Fig. S3A). The CART cytotoxicity was also evaluated by firefly luciferase reporter system assay. The cell lines A549-FFLuc and H460-FFLuc were co-cultured with CD147-CART cells or PBMCs in 96-well plate at the indicated E:T ratios for 6 h. The result of microscopic observations was consistent with the former result in LDH release assay (Fig. S3B, C). FFluc reporter system assay demonstrated that the anti-tumor activity of CD147-CART cells was significantly higher than that of PBMCs, even at E:T ratio of 1:1 (Fig. S3C). Meanwhile, the co-culture supernatant was collected to detect cytokine secreted by CD147-CART cells against tumor cells. Flow cytometry results suggested that CD147-CART secreted more cytokines in the killing tumor cells A549 (Fig. 4D), H460 (Fig. 4E), and H2170 (Fig. 4F) compared with PBMCs, including IL-2, IL-4, IL-6, TNF-α and IFN-γ. In addition, IL-17A and IL-10 secretion were higher in CD147-CART group in some cases (Fig. 4D–F). In short, our findings show that CD147-CART has robust cytotoxicity and cytokine production, suggesting a strong anti-tumor activity against NSCLC tumor cells.

CD147-CART cells show potent anti-tumor activity against NSCLC in xenograft mouse models in vivo

Our *in vitro* experiments showed a strong anti-tumor activity of CD147-CART cells against NSCLC tumor cells. To further investigate the efficacy of CD147-CART cells against NSCLC *in vivo*, the BALB/c nude mice were used to construct the CDX and PDX models. For CDX model, the mice were injected subcutaneously with 2×10^6 A549-FFluc cells in 100 μl sterile PBS. After two weeks, the mice were averagely divided into three groups according to the tumor size. One group of mice received only 2×10^6 PBMCs suspended in 50 μl PBS, one group with 2×10^6 CD147-CART cells suspended in 50 μl PBS, those in the control group underwent the same injection with 50 μl PBS simultaneously. The treatment was performed by intratumoral injection twice a week for a total of four times (Fig. 5A). BMI revealed that CD147-CART administration inhibited tumor growth (Fig. 5B). The tumor volume curve illustrated that the difference of tumor volume in three groups began to expand gradually on day 5, and the tumor volume of CD147-CART group appeared more significant decrease than that of other groups on day 11 and day 13 (Fig. 5C). The mouse weight of all groups have been on rise, especially in CD147-CART group (Fig. 5D), which indicated that CD147-CART helped to improve the health status of mice. The final results of tumor morphology, tumor weight and tumor volume confirmed that CD147-CART cells obviously inhibited tumor growth (Fig. 5E–G). TUNEL assay showed that tumor tissues in CD147-CART group presented larger areas of cell apoptosis than that in other groups (Fig. 6A). Ki67 was stained to evaluate the proliferation of tumor cells, which manifested that CD147-CART treatment significantly inhibited cell proliferation compared with PBS and PBMC groups (Fig. 6B, C). Moreover, CD147-CART group have more CD3+ T cells and CD8+ T cells than PBMC group (Fig. 6D, E). Tumor infiltrating CD8+ T cells released a large number of cytokines, including IL-2, TNF-α, and IFN-γ (Fig. 6F). H&E analysis revealed that no pathologic change was observed in heart, liver, spleen, lung, kidney, and intestines in CD147-

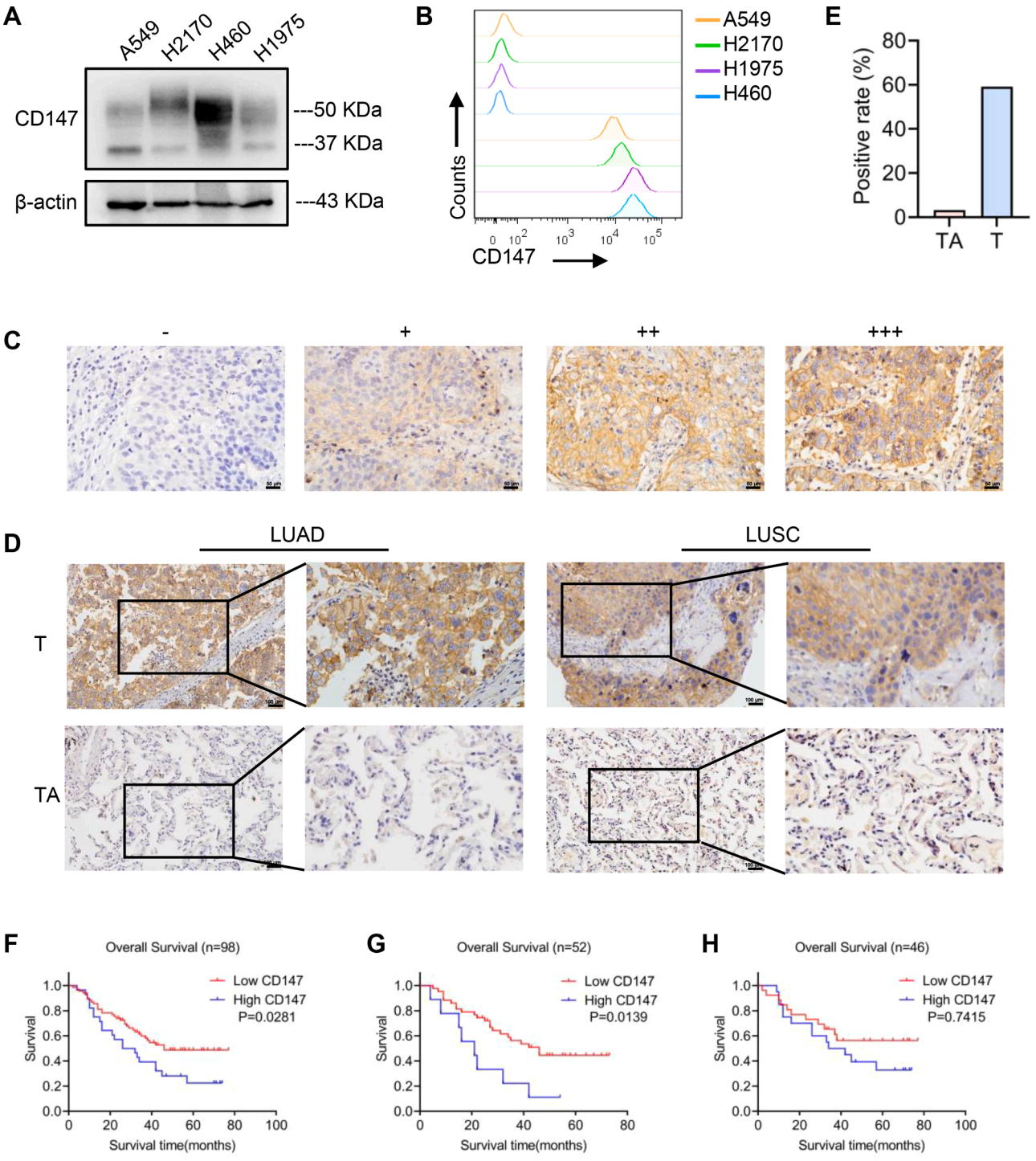

Fig. 2. CD147 expression was detected in NSCLC cell lines and tissues. **A, B** CD147 expression of A549, H2170, H460, and H1975 cells was detected by western blotting and flow cytometry. **C** The expression level of CD147 was classified with "–'', "+'', "++'' and "+++'' in terms of the staining intensity and density of each sample in NSCLC tissues; scale bar = 50 μm. **D** IHC staining showed the expression of CD147 in NSCLC (LUAD and LUSC) tissues (T) and tumor-adjacent tissues (TA); scale bar = 100 μm. **E** The difference of CD147-positive rate between NSCLC tissues (T, $n = 98$) and tumor-adjacent tissues (TA, $n = 92$) was analyzed by Chi-square test (***$P < 0.001$). **F-H** OS rates of high and low CD147 in NSCLC (F), LUAD (G), and LUSC (H) were determined by Kaplan-Meier analysis.

CART groups, which is consistent with the results of PBS and PBMC groups (Fig. 6G). Collectively, our data demonstrate that CD147-CART cells have strong anti-tumor activity against NSCLC cells *in vivo* and no adverse side effects.

Considering the limitations of CDX model, PDX model was constructed to mimic tumor environment and preserve patient characteristic, including heredity, histology, and phenotype. The mice were transplanted with CD147-positive NSCLC tumor tissues, which was identified by IHC staining (Fig. S2B). At 42 days post-inoculation, tumor-bearing mice were averagely divided into two groups according to the tumor size, which were treated with 2×10^6 PBMCs and 2×10^6 CD147-CART suspended in 50 μl PBS intratumorally every three days for a total of three times (Fig. 7A). Under the treatment of CD147-CART cells, tumor volume decreased gradually, which significantly lower

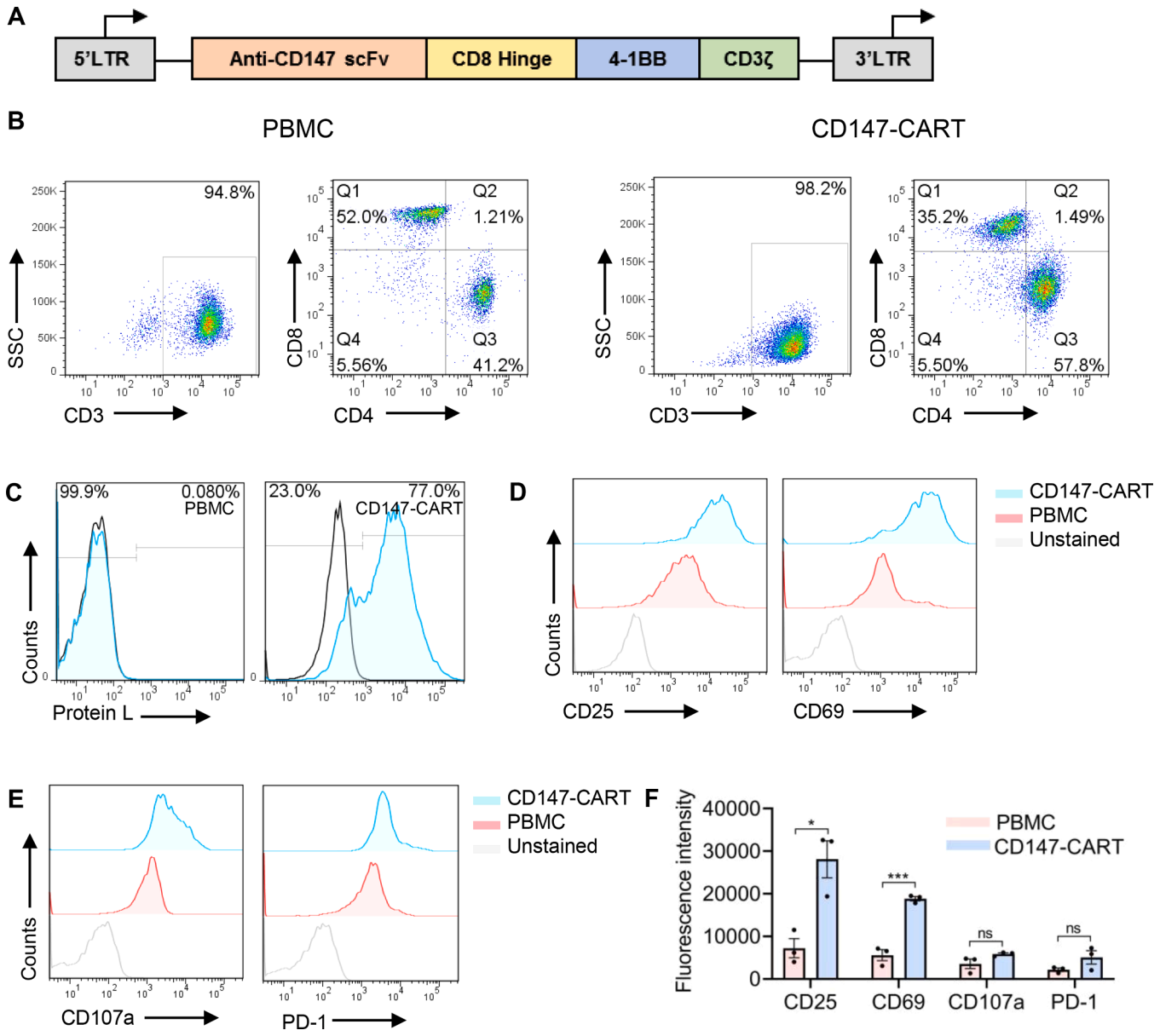

Fig. 3. The generation and phenotype of CD147-CART cells. **A** Schematic outline of CD147-CAR. **B** The cell subtype of CD147-CART cells and PBMCs were detected by flow cytometry using anti-CD3, anti-CD4, and anti-CD8 antibodies. **C** The transfection efficiency of CD147-CART cells was detected by flow cytometry using anti-protein L antibody. **D, E** The phenotypes of CD147-CART cells and PBMCs were detected by flow cytometry using anti-CD25, anti-CD69, anti-CD107a, and anti-PD-1 antibodies. **F** The phenotypes of CD147-CART cells and PBMCs from three independent donors were quantified by fluorescence intensity. Data are presented as mean ± SEM (*$P < 0.05$, ***$P < 0.001$, ns: not significant, $n = 3$ independent experiments).

than that in PBMC group on day 10 (Fig. 7B). There was no significant difference in body weight between the two groups (Fig. 7C). At the end of the treatment, all the mice were sacrificed after anesthesia (Fig. 7D) and the tumor masses were removed from the mice (Fig. 7E). The tumor weight was lower in the CD147-CART group than in PBMC group (Fig. 7F). The consistent result was also obtained in tumor volume between the two groups (Fig. 7G). In the meanwhile, TUNEL assay showed that tumor tissues in CD147-CART group existed massive apoptosis compared with PBMC group (Fig. 7H). Ki67 staining indicated that CD147-CART treatment significantly inhibited cell proliferation (Fig. 7I, J). Moreover, there were more CD3+ and CD8+ T cell infiltration in CD147-CART group than in PBMC group (Fig. 7K, L), which is consistent with the results of CDX model. Together, our findings determine that CD147-CART immunotherapy is effective and safe in CDX and PDX models, which is an ideal and promising medical patch for treating NSCLC.

Discussion

Although many studies on the treatment of NSCLC with CART have been reported, there is still no clinical application of CART drugs for NSCLC treatment until now. The main obstacle of CART immunotherapy for NSCLC is absence of a specific target, like CD19 is overexpressed by the vast majority of B-cell malignancies [35,36]. Therefore, a specific target is particularly important for CART immunotherapy.

Accumulating evidence has verified that CD147 plays a crucial role in tumor progression and prognosis [33,34]. In our study, CD147 is proved to be a potential target, which is highly expressed in NSCLC and almost not expressed in tumor-adjacent tissues. Meanwhile, high CD147 expression is closely associated with poor OS in NSCLC patients. Our previous study shows that anti-CD147 antibody, metuzumab, has prominent antibody-dependent cellular cytotoxicity and inhibits tumor growth without adverse effects [26,37]. An advanced clinical trial

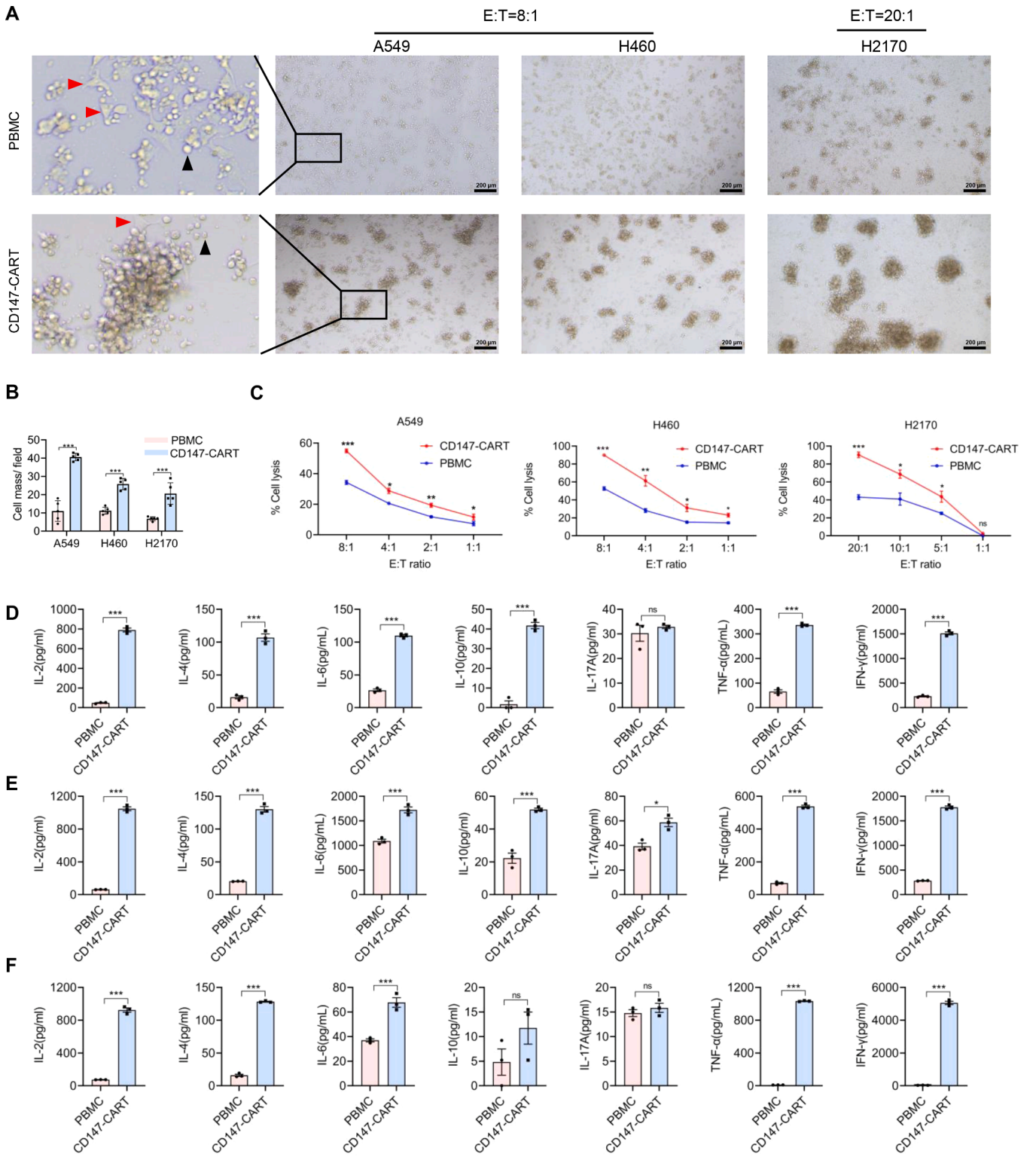

Fig. 4. CD147-CART cells specifically kill NSCLC cells *in vitro*. **A** The co-culture of CD147-CART cells or PBMCS and NSCLC cells (A549, H460 and H2170) at the indicated E:T ratios were observed by microscope; Scale bar = 200 μm. The red arrows denote the NSCLC cell A549, and the black arrows denote PBMCs or CD147-CART cells. **B** The cell masses generated in tumor-killing process were counted and analyzed in five independent fields of each group. Data are presented as mean ± SEM (***$P < 0.001$, $n = 5$ independent experiments). **C** *In vitro* killing assays of CD147-CART cells and PBMCs in A549, H460 and H2170 cell lines were performed at the different E:T ratios. Data are presented as mean ± SEM (*$P < 0.05$, **$P < 0.01$, ***$P < 0.001$, ns: not significant, $n = 3$ independent experiments). **D-F** Cytokine secretion of CD147-CART cells and PBMCs were detected using the co-culture supernatant; A549 cells at an E:T ratio of 8:1(D), H460 cells at an E:T ratio of 8:1(E), and H2170 cells at an E:T ratio of 20:1(F). Data are presented as mean ± SEM (*$P < 0.05$, **$P < 0.01$, ***$P < 0.001$, ns: not significant, $n = 3$ independent experiments).

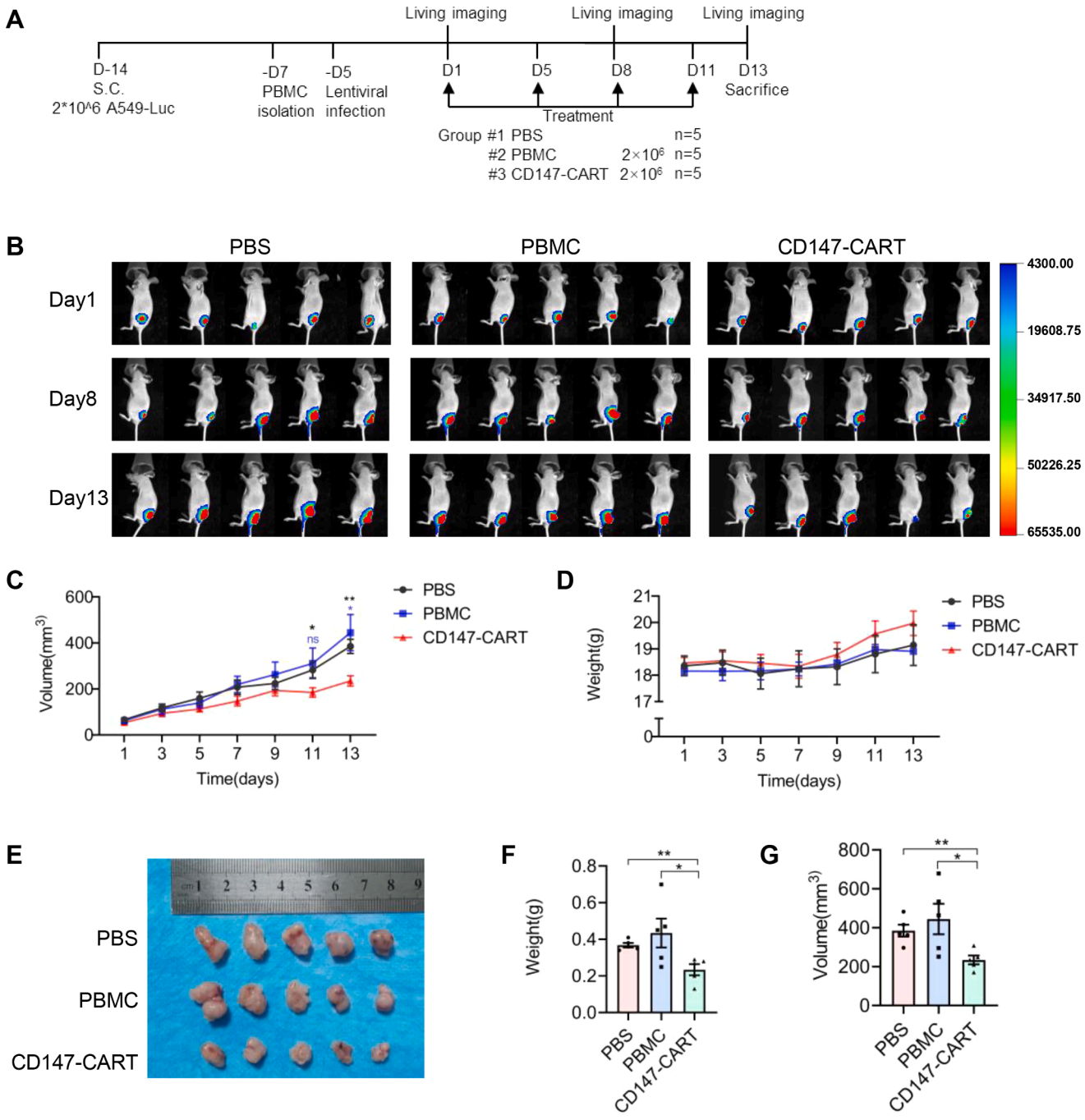

Fig. 5. CD147-CART cells show potent anti-tumor activity against NSCLC in CDX models. **A** Schematic representation of CDX model treatment. **B** BMI of mice were obtained by injection with D-Luciferin potassium salt on day 1, 8 and 13. **C, D** The dynamic curves of tumor volume and mouse weight were measured every two days. Data are presented as mean ± SEM (*$P < 0.05$, **$P < 0.01$, ns: not significant, $n = 5$). **E** A tumor formation assay was performed by injecting A549-FFluc cells into nude mice. **F, G** The tumor weight and tumor volume were quantified in PBS group, PBMC group, and CD147-CART group. Data are presented as mean ± SEM (*$P < 0.05$, **$P < 0.01$, $n = 5$).

reports that ^{131}Iodine (^{131}I) metuximab injection targeting CD147 exhibits a good therapeutic effect in the treatment of hepatocellular carcinoma [25,38]. These studies further suggest that CD147 is a promising tumor antigen, which can be used as a potential target for CART immunotherapy in NSCLC.

Traditional antibody drugs for NSCLC exist a longer half-life, and drug effect lasts several weeks, such as nivolumab, bevacizumab, atezolizumab, compared with that of small molecule drugs [4,39,40]. However, CART cells have obvious advantage in maintaining long-term effective treatment owing to rapid proliferation and differentiate into memory T cells [10,41]. A clinical study shows that CART targeting B-cell maturation antigen for the treatment of multiple myeloma maintains up to 1 year in patients after the infusion [42]. Our animal study demonstrates that CD3+ and CD8+ human T cells still exist in the tumor tissues at the end of the treatment, which is consistent with the result of previous clinical researches.

CART immunotherapy is one of the adoptive cell transfer therapies. Compared with tumor infiltrating lymphocytes, T cell receptor cells and cytokine-induced killer, the most major advantage of CART cells is free from MHC restrictions [43]. CART cells do not need the expression and

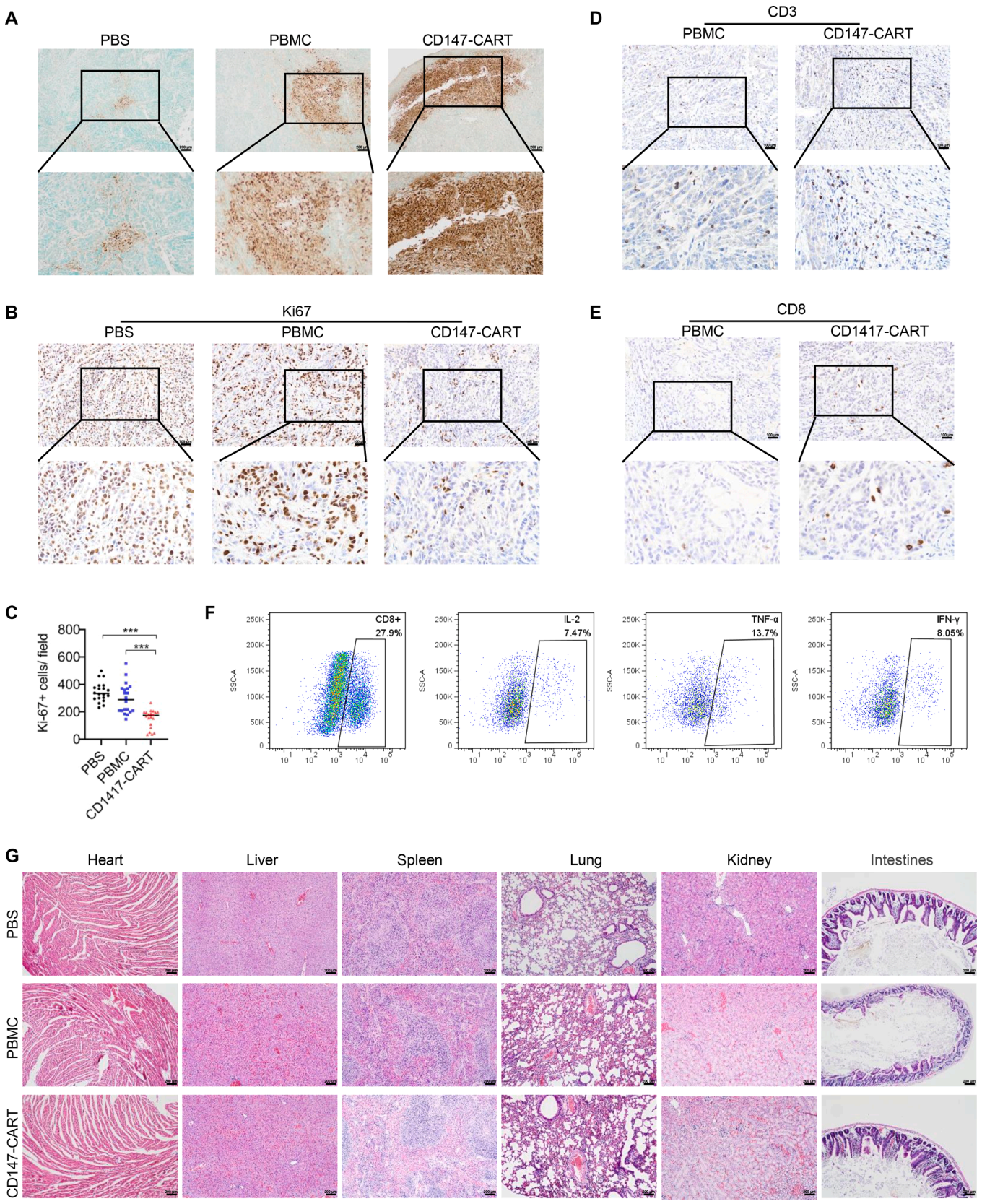

Fig. 6. The pathologic analysis of CDX model. **A** The cell apoptosis in tumor tissues was evaluated using TUNEL Assay Kit; Scale bar = 200 μm. **B** Ki67-positive tumor cells in tumor tissues were evaluated by IHC staining; Scale bar = 100 μm. **C** Ki67-positive tumor cell numbers in 20 random fields (20 dots from 5 mice, 4 dots/mouse) in each group were counted and analyzed. Data are presented as mean ± SEM (***$p < 0.001$, $n = 20$ independent experiments). **D, E** CD3+ T cells (d) and CD8+ T cells (e) in tumor tissues were evaluated by IHC staining; Scale bar = 100 μm. **F** The secretion of IL-2, TNF-α, and IFN-γ in tumor infiltrating CD8+ T cells was analyzed by flow cytometry. **G** The lesion of heart, liver, spleen, lung, kidney, and intestines among PBS, PBMC, and CD147-CART groups were detected by H&E staining; Scale bar = 200 μm.

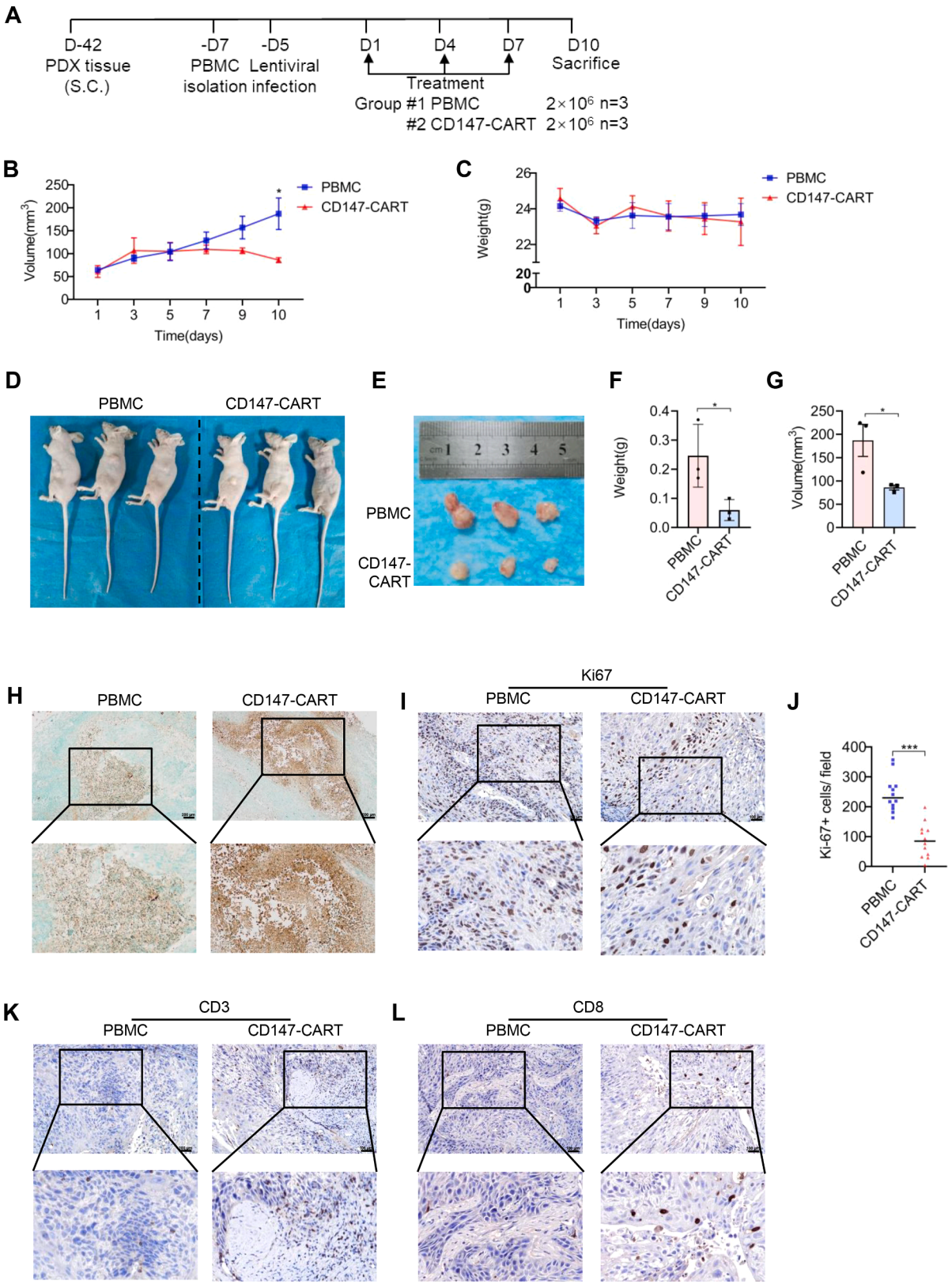

Fig. 7. CD147-CART cells show potent anti-tumor activity against NSCLC in PDX models. **A** Schematic representation of PDX model treatment. **B, C** The dynamic curves of tumor volume and mouse weight were measured. Data are presented as mean ± SEM (*$P < 0.05$, $n = 3$). **D, E** The mice appearance and tumor morphology were shown. **F, G** The tumor weight and tumor volume were quantified in PBMC group and CD147-CART group. Data are presented as mean ± SEM (*$P < 0.05$, $n = 3$). **H** The cell apoptosis in tumor tissues was evaluated using TUNEL Assay Kit; Scale bar = 200 μm. **I** Ki67-positive tumor cells in tumor tissues were evaluated by IHC staining; Scale bar = 100 μm. **J** Ki67-positive tumor cell numbers in 12 random fields (12 dots from 3 mice, 4 dots/ mouse) in each group were counted and analyzed. Data are presented as mean ± SEM (***$p < 0.001$, $n = 12$ independent experiments). **K, L** CD3+ T cells (k) and CD8+ T cells (l) in tumor tissues were evaluated by IHC staining; Scale bar = 100 μm.

identity of MHC, and its extracellular scFv fragment directly binds target antigen to kill tumor cells [13,44,45]. Therefore, CART cells effectively avoid the immune escape caused by down-regulation or loss of MHC molecules. In our study, *in vivo* and *in vitro* experiments confirmed that CD147-CART cells kill tumor cells more effectively compared with PBMC group, which exhibits a strong anti-tumor activity and cytokine production.

In clinical practice, avoiding adverse CRS is also an essential factor of CART therapy. Compared with intravenous administration, intratumoral treatment is a safe strategy, which not only avoids severe CRS, but also contributes to the infiltration of CART cells into tumor tissues. Previous study demonstrates that B7-H3.BB.z-CAR cells administered intratumorally mediate potent antitumor effects against cerebral ATRT xenografts in mice, with faster kinetics, greater potency and reduced systemic levels of inflammatory cytokines compared to CART cells administered intravenously [46]. A clinical trial also shows that intratumoral injections of mRNA c-Met-CART cells are well tolerated and evoke an inflammatory response within tumors [47]. In our study, intratumoral administration for CD147-CART cells was conducted in tumor-bearing mice, which showed an effective anti-tumor activity and no adverse side effects. These results tentatively suggest that, intratumoral administration for CD147-CART cells is safe and considerable to treat NSCLC, which can avoid the toxic or side effects on other CD147-positive normal tissues, including gastrointestinal tract, kidneys, and genitals. However, the humanized CD147 mouse is still needed to further evaluate the safety of CD147-CART in NSCLC treatment, including adverse CRS and organ lesion.

Although CD147-CART cells show a better therapeutic effect against NSCLC, there are still a few issues we need to address. In our study, we failed to provide survival data for the mice and the number of PDX models was small due to the tumorigenicity and homogeneity of the tumor. Moreover, the side effects of CD147-CART cells were not thoroughly evaluated, including serum cytokines, neurotoxicity, and reproductive toxicity. Meanwhile, we need to enhance the proliferation and persistence of CART cells, which is vital of durable remission and preventing recurrence in NSCLC. Embedding cytokine domain and co-stimulatory domain into CAR structure not only enhances CART cell proliferation, but also promotes CART cells to differentiate into memory T cells [48–54], which will improve the therapeutic effect of CART cells. In addition, remodeling the tumor microenvironment is also crucial to the therapeutic effect of CART cells. The combination of CART cells and PD-1 inhibitor or CTLA-4 inhibitor is a good strategy to prevent immunosuppression, which enables CART cells to maximize their killing effect [55–57].

Conclusions

In summary, CD147 is proved to be a specific tumor antigen of NSCLC, and we construct CART cells targeting CD147 to treat NSCLC. Our data demonstrate that CD147-CART cells have a strong anti-tumor activity against NSCLC *in vitro and in vivo*. These results indicate that CD147-CART immunotherapy is a safe and efficient strategy for NSCLC, which provides a theoretical basis for the clinical treatment of NSCLC with CD147-CART cells.

CRediT authorship contribution statement

Xiao-Hong Chen: Conceptualization, Investigation, Writing – review & editing. **Ruo Chen:** . **Ming-Yan Shi:** . **Ruo-Fei Tian:** Software, Methodology. **Hai Zhang:** Software, Methodology. **Zhi-Qian Xin:** Software, Methodology. **Zhi-Nan Chen:** Conceptualization, Writing – review & editing, Supervision. **Ke Wang:** Writing – review & editing, Supervision.

Declaration of Competing Interest

The authors declare that they have no competing interests.

Acknowledgments

We thank Tianjiao Zhang, Haijiao Yang, and Bin Wang for technical help in cell and animal experiments.

Funding

This work was supported by a grant from the National Natural Science Foundation of China (82002425) and Young Elite Scientist Sponsorship Program by Cast of China Association for Science and Technology (YESS20200011).

Availability of data and materials

All data in our study are included in the article or uploaded as supplementary information.

Ethics approval and consent to participate

This study was approved by the ethics committees of Fourth Military Medical University, and the procedures in animal experiments were approved by the Animal Care and Use Committee of Fourth Military Medical University.

Consent for publication

Not applicable.

Author details

1 National Translational Science Center for Molecular Medicine & Department of Cell Biology, Fourth Military Medical University, Xi'an 710032, China

Supplementary materials

Supplementary material associated with this article can be found, in the online version, at doi:10.1016/j.tranon.2021.101309.

References

[1] C.E. DeSantis, K.D. Miller, W. Dale, S.G. Mohile, H.J. Cohen, C.R. Leach, A. Goding Sauer, A. Jemal, R.L. Siegel, Cancer statistics for adults aged 85 years and older, 2019, CA Cancer J. Clin. 69 (6) (2019) 452–467.
[2] F. Bray, J. Ferlay, I. Soerjomataram, R.L. Siegel, L.A. Torre, A. Jemal, Global cancer statistics 2018: GLOBOCAN estimates of incidence and mortality worldwide for 36 cancers in 185 countries, CA Cancer J. Clin. 68 (6) (2018) 394–424.
[3] R.L. Siegel, K.D. Miller, H.E. Fuchs, A. Jemal, Cancer Statistics, 2021, CA Cancer J. Clin. 71 (1) (2021) 7–33.
[4] N. Duma, R. Santana-Davila, J.R. Molina, Non-Small Cell Lung Cancer: epidemiology, Screening, Diagnosis, and Treatment, Mayo Clin. Proc. 94 (8) (2019) 1623–1640.
[5] J.T.C. de Azevedo, A. Mizukami, P.D. Moco, K.C.R. Malmegrim, Immunophenotypic analysis of CAR-T cells, Methods Mol. Biol. 2086 (2020) 195–201.
[6] M. Fukuoka, S. Yano, G. Giaccone, T. Tamura, K. Nakagawa, J.Y. Douillard, Y. Nishiwaki, J. Vansteenkiste, S. Kudoh, D. Rischin, et al., Multi-institutional randomized phase II trial of gefitinib for previously treated patients with advanced non-small-cell lung cancer (The IDEAL 1 Trial) [corrected], J. Clin. Oncol. 21 (12) (2003) 2237–2246.
[7] P. Goldstraw, K. Chansky, J. Crowley, R. Rami-Porta, H. Asamura, W.E. Eberhardt, A.G. Nicholson, P. Groome, A. Mitchell, V. Bolejack, The IASLC Lung Cancer Staging Project: proposals for revision of the tnm stage groupings in the forthcoming (Eighth) edition of the TNM Classification for lung cancer, J. Thorac. Oncol. 11 (1) (2016) 39–51.
[8] F.R. Hirsch, G.V. Scagliotti, J.L. Mulshine, R. Kwon, W.J. Curran, Y.L. Wu, L. Paz-Ares, Lung cancer: current therapies and new targeted treatments, Lancet 389 (10066) (2017) 299–311.

[9] A. Morabito, M.C. Piccirillo, F. Falasconi, G. De Feo, A. Del Giudice, J. Bryce, M. Di Maio, E. De Maio, N. Normanno, F. Perrone, Vandetanib (ZD6474), a dual inhibitor of vascular endothelial growth factor receptor (VEGFR) and epidermal growth factor receptor (EGFR) tyrosine kinases: current status and future directions, Oncologist 14 (4) (2009) 378–390.

[10] K. Newick, S. O'Brien, E. Moon, S.M. Albelda, CAR T cell therapy for solid tumors, Annu. Rev. Med. 68 (2017) 139–152.

[11] A. Steven, S.A. Fisher, B.W. Robinson, Immunotherapy for lung cancer, Respirology 21 (5) (2016) 821–833.

[12] L.B. Kennedy, A.K.S. Salama, A review of cancer immunotherapy toxicity, CA Cancer J. Clin. 70 (2) (2020) 86–104.

[13] C.H. June, CAR T cell immunotherapy for human cancer, Science (2018).

[14] M. Hong, J.D. Clubb, Y.Y. Chen, Engineering CAR-T cells for next-generation cancer therapy, Cancer Cell 38 (4) (2020) 473–488.

[15] L. Labanieh, R.G. Majzner, C.L. Mackall, Programming CAR-T cells to kill cancer, Nat. Biomed. Eng. 2 (6) (2018) 377–391.

[16] J. Zhao, Q. Lin, Y. Song, D. Liu, Universal CARs, universal T cells, and universal CAR T cells, J. Hematol. Oncol. 11 (1) (2018) 132.

[17] J. Qu, Q. Mei, L. Chen, J. Zhou, Chimeric antigen receptor (CAR)-T-cell therapy in non-small-cell lung cancer (NSCLC): current status and future perspectives, Cancer Immunol. Immunother. 70 (3) (2021) 619–631.

[18] C.A. Ramos, H.E. Heslop, M.K. Brenner, CAR-T Cell therapy for lymphoma, Annu. Rev. Med. 67 (2016) 165–183.

[19] E. Drent, R. Poels, R. Ruiter, N. van de Donk, S. Zweegman, H. Yuan, J. de Bruijn, M. Sadelain, H.M. Lokhorst, R.W.J. Groen, et al., Combined CD28 and 4-1BB costimulation potentiates affinity-tuned chimeric antigen receptor-engineered T Cells, Clin. Cancer Res. 25 (13) (2019) 4014–4025.

[20] X. Xin, X. Zeng, H. Gu, M. Li, H. Tan, Z. Jin, T. Hua, R. Shi, H. Wang, CD147/EMMPRIN overexpression and prognosis in cancer: a systematic review and meta-analysis, Sci. Rep. 6 (2016) 32804.

[21] X. Zhu, Z. Song, S. Zhang, A. Nanda, G. Li, CD147: a novel modulator of inflammatory and immune disorders, Curr. Med. Chem. 21 (19) (2014) 2138–2145.

[22] C. Wang, R. Jin, X. Zhu, J. Yan, G. Li, Function of CD147 in atherosclerosis and atherothrombosis, J. Cardiovasc. Transl. Res. 8 (1) (2015) 59–66.

[23] S.N.I. von Ungern-Sternberg, A. Zernecke, P. Seizer, Extracellular matrix metalloproteinase inducer EMMPRIN (CD147) in cardiovascular disease, Int. J. Mol. Sci. 19 (2) (2018).

[24] F. Fei, S. Li, Z. Fei, Z. Chen, The roles of CD147 in the progression of gliomas, Expert Rev. Anticancer Ther. 15 (11) (2015) 1351–1359.

[25] Z.N. Chen, L. Mi, J. Xu, F. Song, Q. Zhang, Z. Zhang, J.L. Xing, H.J. Bian, J.L. Jiang, X.H. Wang, et al., Targeting radioimmunotherapy of hepatocellular carcinoma with iodine (131I) metuximab injection: clinical phase I/II trials, Int. J. Radiat. Oncol. Biol. Phys. 65 (2) (2006) 435–444.

[26] Z. Zhang, Y. Zhang, Q. Sun, F. Feng, M. Huhe, L. Mi, Z. Chen, Preclinical pharmacokinetics, tolerability, and pharmacodynamics of metuzumab, a novel CD147 human-mouse chimeric and glycoengineered antibody, Mol. Cancer Ther. 14 (1) (2015) 162–173.

[27] Z. Tang, C. Li, B. Kang, G. Gao, C. Li, Z. Zhang, GEPIA: a web server for cancer and normal gene expression profiling and interactive analyses, Nucleic Acids Res. 45 (W1) (2017) W98–w102.

[28] B. Győrffy, P. Surowiak, J. Budczies, A. Lánczky, Online survival analysis software to assess the prognostic value of biomarkers using transcriptomic data in non-small-cell lung cancer, PLoS ONE 8 (12) (2013) e82241.

[29] B. Li, E. Severson, J.C. Pignon, H. Zhao, T. Li, J. Novak, P. Jiang, H. Shen, J. C. Aster, S. Rodig, et al., Comprehensive analyses of tumor immunity: implications for cancer immunotherapy, Genome Biol. 17 (1) (2016) 174.

[30] T. Li, J. Fan, B. Wang, N. Traugh, Q. Chen, J.S. Liu, B. Li, X.S. Liu, TIMER: a web server for comprehensive analysis of tumor-infiltrating immune cells, Cancer Res. 77 (21) (2017) e108–e110.

[31] H.Y. Cui, S.J. Wang, F. Song, X. Cheng, G. Nan, Y. Zhao, M.R. Qian, X. Chen, J.Y. Li, F.L. Liu, et al., CD147 receptor is essential for TFF3-mediated signaling regulating colorectal cancer progression, Signal Transduct. Target Ther. 6 (1) (2021) 268.

[32] Di-methylation of CD147-K234 Promotes the Progression of NSCLC by Enhancing Lactate Export.

[33] A. Landras, C. Reger de Moura, F. Jouenne, C. Lebbe, S. Menashi, S. Mourah, CD147 is a promising target of tumor progression and a prognostic biomarker, Cancers (Basel) 11 (11) (2019).

[34] C. Lian, Y. Guo, J. Zhang, X. Chen, C. Peng, Targeting CD147 is a novel strategy for antitumor therapy, Curr. Pharm. Des. 23 (29) (2017) 4410–4421.

[35] M. Mohty, J. Gautier, F. Malard, M. Aljurf, A. Bazarbachi, C. Chabannon, M. A. Kharfan-Dabaja, B.N. Savani, H. Huang, S. Kenderian, et al., CD19 chimeric antigen receptor-T cells in B-cell leukemia and lymphoma: current status and perspectives, Leukemia 33 (12) (2019) 2767–2778.

[36] J.N. Kochenderfer, S.A. Rosenberg, Treating B-cell cancer with T cells expressing anti-CD19 chimeric antigen receptors, Nat. Rev. Clin. Oncol. 10 (5) (2013) 267–276.

[37] F. Peng, H. Li, Q. You, H. Li, D. Wu, C. Jiang, G. Deng, Y. Li, Y. Li, Y. Wu, CD147 as a novel prognostic biomarker for hepatocellular carcinoma: a meta-analysis, Biomed. Res. Int. 2017 (2017), 5019367.

[38] H. Bian, J.S. Zheng, G. Nan, R. Li, C. Chen, C.X. Hu, Y. Zhang, B. Sun, X.L. Wang, S. C. Cui, et al., Randomized trial of [131I] metuximab in treatment of hepatocellular carcinoma after percutaneous radiofrequency ablation, J. Natl. Cancer Inst. 106 (9) (2014).

[39] D.B. Doroshow, M.F. Sanmamed, K. Hastings, K. Politi, D.L. Rimm, L. Chen, I. Melero, K.A. Schalper, R.S. Herbst, Immunotherapy in non-small cell lung cancer: facts and hopes, Clin. Cancer Res. 25 (15) (2019) 4592–4602.

[40] R.S. Herbst, D. Morgensztern, C. Boshoff, The biology and management of non-small cell lung cancer, Nature 553 (7689) (2018) 446–454.

[41] H.J. Jackson, S. Rafiq, R.J. Brentjens, Driving CAR T-cells forward, Nat. Rev. Clin. Oncol. 13 (6) (2016) 370–383.

[42] N. Raje, J. Berdeja, Y. Lin, D. Siegel, S. Jagannath, D. Madduri, M. Liedtke, J. Rosenblatt, M.V. Maus, A. Turka, et al., Anti-BCMA CAR T-cell therapy bb2121 in relapsed or refractory multiple myeloma, N. Engl. J. Med. 380 (18) (2019) 1726–1737.

[43] R. Zhang, Z. Zhang, Z. Liu, D. Wei, X. Wu, H. Bian, Z. Chen, Adoptive cell transfer therapy for hepatocellular carcinoma, Front. Med. 13 (1) (2019) 3–11.

[44] S. Ma, X. Li, X. Wang, L. Cheng, Z. Li, C. Zhang, Z. Ye, Q. Qian, Current progress in CAR-T cell therapy for solid tumors, Int. J. Biol. Sci. 15 (12) (2019) 2548–2560.

[45] R.D. Leone, J.D. Powell, Metabolism of immune cells in cancer, Nat. Rev. Cancer (2020).

[46] J. Theruvath, E. Sotillo, C.W. Mount, C.M. Graef, A. Delaidelli, S. Heitzeneder, L. Labanieh, S. Dhingra, A. Leruste, R.G. Majzner, et al., Locoregionally administered B7-H3-targeted CAR T cells for treatment of atypical teratoid/rhabdoid tumors, Nat. Med. 26 (5) (2020) 712–719.

[47] J. Tchou, Y. Zhao, B.L. Levine, P.J. Zhang, M.M. Davis, J.J. Melenhorst, I. Kulikovskaya, A.L. Brennan, X. Liu, S.F. Lacey, et al., Safety and efficacy of intratumoral injections of chimeric antigen receptor (CAR) T cells in metastatic breast cancer, Cancer Immunol. Res. 5 (12) (2017) 1152–1161.

[48] Z. Zhao, M. Condomines, S.J.C. van der Stegen, F. Perna, C.C. Kloss, G. Gunset, J. Plotkin, M. Sadelain, Structural design of engineered costimulation determines tumor rejection kinetics and persistence of CAR T cells, Cancer Cell 28 (4) (2015) 415–428.

[49] O.O. Yeku, R.J. Brentjens, Armored CAR T-cells: utilizing cytokines and pro-inflammatory ligands to enhance CAR T-cell anti-tumour efficacy, Biochem. Soc. Trans. 44 (2) (2016) 412–418.

[50] M. Chmielewski, A.A. Hombach, H. Abken, Of CARs and TRUCKs: chimeric antigen receptor (CAR) T cells engineered with an inducible cytokine to modulate the tumor stroma, Immunol. Rev. 257 (1) (2014) 83–90.

[51] M. Chmielewski, H. Abken, TRUCKs: the fourth generation of CARs, Expert Opin. Biol. Ther. 15 (8) (2015) 1145–1154.

[52] D.A. Vignali, V.K. Kuchroo, IL-12 family cytokines: immunological playmakers, Nat. Immunol. 13 (8) (2012) 722–728.

[53] T. Floros, A.A. Tarhini, Anticancer cytokines: biology and clinical effects of interferon-α2, Interleukin (IL)-2, IL-15, IL-21, and IL-12, Semin. Oncol. 42 (4) (2015) 539–548.

[54] L. Zhang, R.A. Morgan, J.D. Beane, Z. Zheng, M.E. Dudley, S.H. Kassim, A.V. Nahvi, L.T. Ngo, R.M. Sherry, G.Q. Phan, et al., Tumor-infiltrating lymphocytes genetically engineered with an inducible gene encoding interleukin-12 for the immunotherapy of metastatic melanoma, Clin. Cancer Res. 21 (10) (2015) 2278–2288.

[55] I. Scarfò, M.V. Maus, Current approaches to increase CAR T cell potency in solid tumors: targeting the tumor microenvironment, J. Immunother. Cancer 5 (2017) 28.

[56] T. Wu, Y. Dai, Tumor microenvironment and therapeutic response, Cancer Lett. 387 (2017) 61–68.

[57] M. Binnewies, E.W. Roberts, K. Kersten, V. Chan, D.F. Fearon, M. Merad, L. M. Coussens, D.I. Gabrilovich, S. Ostrand-Rosenberg, C.C. Hedrick, et al., Understanding the tumor immune microenvironment (TIME) for effective therapy, Nat. Med. 24 (5) (2018) 541–550.